molecules

MDPI

Article

The DEPTQ$^+$ Experiment: Leveling the DEPT Signal Intensities and Clean Spectral Editing for Determining CH_n Multiplicities

Peter Bigler *, Camilo Melendez and Julien Furrer *

Departement für Chemie, Biochemie und Pharmazie, Universität Bern, Freiestrasse 3, CH-3012 Bern, Switzerland; camilo.melendez@dcb.unibe.ch

* Correspondence: biglermeier@bluewin.ch (P.B.); julien.furrer@dcb.unibe.ch (J.F.)

Abstract: We propose a new ^{13}C DEPTQ$^+$ NMR experiment, based on the improved DEPTQ experiment, which is designed to unequivocally identify all carbon multiplicities (Cq, CH, CH_2, and CH_3) in two experiments. Compared to this improved DEPTQ experiment, the DEPTQ$^+$ is shorter and the different evolution delays are designed as spin echoes, which can be tuned to different $^1J_{CH}$ values; this is especially valuable when a large range of $^1J_{CH}$ coupling constants is to be expected. These modifications allow (i) a mutual leveling of the DEPT signal intensities, (ii) a reduction in *J* cross-talk in the Cq/CH spectrum, and (iii) more consistent and cleaner CH_2/CH_3 edited spectra. The new DEPTQ$^+$ is expected to be attractive for fast ^{13}C analysis of small-to medium sized molecules, especially in high-throughput laboratories. With concentrated samples and/or by exploiting the high sensitivity of cryogenically cooled ^{13}C NMR probeheads, the efficacy of such investigations may be improved, as it is possible to unequivocally identify all carbon multiplicities, with only one scan, for each of the two independent DEPTQ$^+$ experiments and without loss of quality.

Keywords: NMR; ^{13}C; DEPTQ; DEPTQ$^+$; spectral editing; *J*-cross talk; signal intensity leveling

Citation: Bigler, P.; Melendez, C.; Furrer, J. The DEPTQ$^+$ Experiment: Leveling the DEPT Signal Intensities and Clean Spectral Editing for Determining CH_n Multiplicities. *Molecules* **2021**, *26*, 3490. https://doi.org/10.3390/molecules26123490

Academic Editor: Antony J. Williams

Received: 6 May 2021
Accepted: 27 May 2021
Published: 8 June 2021

1. Introduction

Two-dimensional heteronuclear NMR techniques for ^{13}C assignment have long been considered extremely powerful since they are much more sensitive than, e.g., one-dimensional (1D) ^{13}C spectral editing experiments [1], and the corresponding spectra contain a lot of information. Nevertheless, "old" 1D experiments such as SEFT [2], APT [3] and PENDANT [4,5], refocused variants of INEPT [6], DEPT [7,8], DEPTQ [9–11] and SEMUT [12], continue to be very useful for routine applications [13]. A likely reason for the popularity of these 1D experiments is the rather low resolution achieved in the indirect dimension (^{13}C) with 2D heteronuclear experiments, such as HSQC [14], HMBC [15–17] or LR-HSQMBC [18], under standard experimental conditions, thus potentially preventing the unambiguous differentiation between closely spaced ^{13}C resonances. In principle, this problem can easily be alleviated [19,20] but the required experiments/methods can only be routinely applied to a certain extent, as they require in-depth knowledge of theoretical and experimental NMR spectroscopy.

One-dimensional ^{13}C experiments such as APT [2], PENDANT [4,5], and DEPTQ [9–11], provide information about both quaternary and protonated carbons in the spectra, with the signals of Cq and CH_2 carbons being 180° out-of-phase with respect to the signals of CH and CH_3 carbons. Among those experiments, the DEPTQ encompasses all the known advantages of the basic DEPT experiment but includes the signals of quaternary carbons. The DEPT pulse sequences, thanks to their marked insensitivity to experimental parameters compared to other experimental schemes, have proven to be the experiments of choice for obtaining the chemical shift and multiplicity information for all types of protonated carbons [8]. Additionally, a version of DEPTQ with the length of the initial ^1H pulse adjusted accordingly allows simplified spectral editing: with this first and the final

proton pulse adjusted to 45° and 90°, respectively, for a DEPTQ90 ($DEPTQ90_{45}$) and adjusted to 90° and 135°, respectively, for a DEPTQ135 ($DEPTQ135_{90}$), the intensities of CH signals are equal in both experiments, since they are reduced to 70% of their maximum value with the $DEPTQ90_{45}$ experiment. Thus, subtracting the $DEPTQ90_{45}$ and the $DEPTQ135_{90}$ from each other yields a CH_2/CH_3 edited spectrum with the signals of the two carbon types in opposite phase [11]. The DEPTQ90 spectrum shows exclusively, and with opposite phase, the signals of Cq and CH.

Therefore, although no Cq-. CH-, CH_2- and CH_3-only spectra result, the pairwise editing with opposite signs for the signals of different multiplicities allows unambiguous spectral editing with only two experiments, and conceivably, with only one scan each, e.g., for highly concentrated samples [11].

Experimentally, we found that with the DEPTQ experiment, the editing filter quality in the Cq/CH and CH_2/CH_3 subspectra is not satisfactory, with a breakthrough of many artifacts originating from other CH_n multiplicities [13]. We also observed that for molecules possessing large ranges of $^1J_{CH}$ coupling constants, DEPTQ135 spectra and edited subspectra are obtained, with missing or very weak signals, especially CH_3 or alkyne CH groups (Figure 1). For instance, in the $DEPTQ135_{90}$ spectrum of 4-methyl-*N*,*N*-di(prop-2-yn-1-yl)aniline, the resonance of the methyl group C8 at 20.6 ppm is almost invisible (Figure 1). While the $DEPTQ90_{45}$ spectrum appears satisfactory, the edited CH_2/CH_3 subspectrum is misleading, as the resonance of the methyl group C8 at 20.6 ppm is absent. We thought it useful to develop a modified DEPTQ scheme for obtaining consistent DEPTQ and edited subspectra for all classes of molecules. This could potentially be very attractive for rapid ^{13}C analysis of newly synthesized or isolated compounds, especially for high-throughput NMR analysis.

In this article, we present a new pulse sequence, $DEPTQ^+$, possessing all these attributes, and compare it with the modified DEPTQ experiment, designed to unequivocally identify all carbon multiplicities (Cq, CH, CH_2, and CH_3) in two experiments. We show both theoretically and experimentally that the $DEPTQ^+$ pulse sequence always provides unambiguous DEPTQ spectra with a leveling of all carbon intensities. This generally results in processed spectra with a clean separation of the Cq and CH signals in one spectrum and the CH_2 and CH_3 signals in the other, with both spectra showing the signals of the two carbon species in opposite phases. It must be emphasized, however, that these properties only come into play and are relevant for molecules possessing a large range of $^1J_{CH}$ coupling constants.

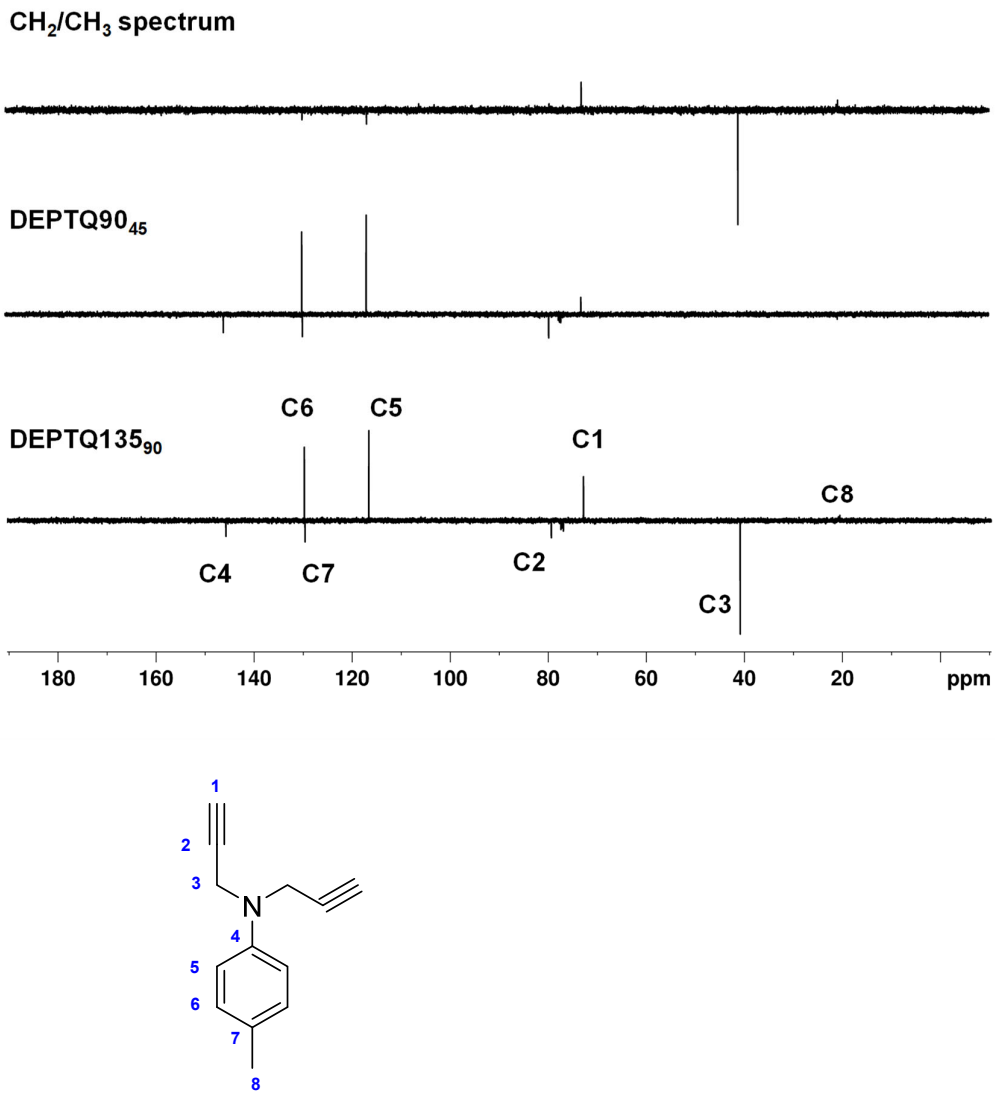

Figure 1. 4-methyl-*N*,*N*-di(prop-2-yn-1-yl)aniline and carbon numbering and DEPTQ135$_{90}$, DEPTQ90$_{45}$, and the difference between DEPTQ135$_{90}$ and DEPTQ90$_{45}$ spectra of ~30 mg of 4-methyl-*N*,*N*-di(prop-2-yn-1-yl)aniline dissolved in 0.7 mL $CDCl_3$. The delay δ was set to 2.70 ms, adjusted for a coupling constant $^1J_{CH}$ of 185 Hz. The relaxation delay was 2 s, the NOE building period 1 s. All other parameters are identical to those described in the Materials and Methods section.

2. Results and Discussion

2.1. Theory

2.1.1. Original DEPTQ Pulse Sequence

Despite their known tolerance to the experimental parameters, edited DEPTQ spectra may show undesirable residual CH_n signals from "wrong" carbon types, a phenomenon termed dubbed *J* cross-talk [21]. These signals arise, among other things, with non-ideally adjusted delays and occur for both the coherences resulting from initial ^1H- and from ^{13}C-polarization. These signals are particularly troublesome in the pairwise edited CH_n spectra, as they can lead to misinterpretation, particularly if the editing is performed in an automatic or semi-automatic way and with samples containing several, differently concentrated components [22–27]. Therefore, this study predominantly focuses on suppressing remaining CH_n signals in the different subspectra as efficiently as possible.

The general condition $\delta \neq 1/(2 * {}^{1}J_{CH})$ is assumed in the following first product operator treatments of the original DEPTQ pulse sequence (Figure 2). For simplicity, ^{1}H- and ^{13}C-shift evolutions during the delays δ and the gradients G_1–G_3 used in practice are not considered (the overall result is identical, except that only one of the ^{13}C magnetization terms at coherence level −1, C^{-}, is detected if the PFGs are considered). We use here the bracket notations proposed by Mateescu and Valeriu [28].

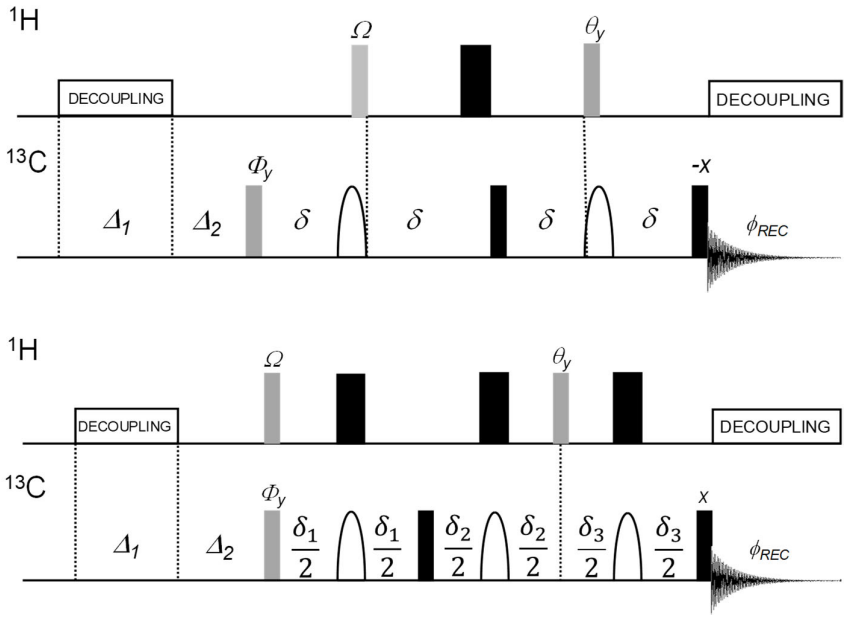

Figure 2. DEPTQ [11] (**top**) and DEPTQ^{+} pulse sequences (**bottom**) for editing CH_n multiplicities. The first adjustable proton pulse Ω and the editing pulse θ are set to 45° and 90°, respectively, for a DEPTQ90 (DEPTQ90$_{45}$) and to 90° and 135°, respectively, for a DEPTQ135 (DEPTQ135$_{90}$), and the delay δ is adjusted to $1/(2 * {}^{1}J_{CH})$. The DEPTQ90$_{45}$ spectrum, showing exclusively the Cq and CH signals with opposite phases, and the DEPTQ135$_{90}$ spectrum, are subtracted from each other results in a CH_2/CH_3 edited spectrum with the signals of the two carbon types with opposite phases.[11] The ^{13}C 180° (refocusing) pulses are composite smoothed chirp pulses (2 ms total duration, 60 kHz sweep width). The initial ^{13}C 90° pulse may be replaced by a variable φ pulse, adjustable for maximum sensitivity (Ernst angle). An additional 90° ^{13}C pulse prior to data acquisition reestablishes the residual ^{13}C-z magnetization left with the initial ^{13}C pulse. In the DEPTQ^{+}, compared to the original DEPTQ version [10,11], the first evolution delay δ is omitted, and the remaining three evolution periods are defined as spin echoes, thus allowing different values for δ_1, δ_2, and δ_3 to be used. The first adjustable proton pulse Ω and the editing pulse θ are set to 45° and 90°, respectively, for a DEPTQ^{+}90 (DEPTQ^{+}90$_{45}$) and to 90° and 45°, respectively, for a DEPTQ^{+}45 (DEPTQ^{+}45$_{90}$).

Quaternary Carbons

The first ^{13}C pulse φ is set arbitrarily (Ernst angle)

$$\begin{aligned}[z] \xrightarrow{\emptyset^\circ yC} & cos\emptyset[z] + sin\emptyset[x] \xrightarrow{\delta} cos\emptyset[z] + sin\emptyset[x] \xrightarrow{\Omega^\circ xH} \xrightarrow{180^\circ xC} \xrightarrow{\delta} - cos\emptyset[z] \\ & + sin\emptyset[x] \xrightarrow{180^\circ xH} \xrightarrow{90^\circ xC} cos\emptyset[y] + sin\emptyset[x] \xrightarrow{\delta} cos\emptyset[y] \\ & + sin\emptyset[x] \xrightarrow{180^\circ xC} \xrightarrow{\theta^\circ yH} - cos\emptyset[y] + sin\emptyset[x] \xrightarrow{\delta} \xrightarrow{90^\circ - xC} cos\emptyset[z] \\ & + sin\emptyset[x] \end{aligned} \quad (1)$$

Of course, the outcome for quaternary carbons is identical in both experiments, DEPTQ135$_{90}$, Ω = 90° and DEPTQ90$_{45}$, Ω = 45°, irrespective of the length of the proton pulse θ.

DEPTQ135, Ω = 90°, θ = 135°

Subsequently, the following abbreviations will be used:

$$c = \cos \pi J\delta \text{ and } s = \sin \pi J\delta \qquad c2 = \cos 2\pi J_{CH}\delta \text{ and } s2 = \sin 2\pi J_{CH}\delta$$

For the observable signals originating from the polarization transfer from ^{1}H to ^{13}C (DEPT135), we obtain [7,8,29]:

1. CH groups

$$\begin{aligned}[1z] \xrightarrow{\emptyset^\circ yC} \xrightarrow{\delta} [1z] \xrightarrow{90^\circ xH} \xrightarrow{180^\circ xC} -[1y] \xrightarrow{\delta} s[zx] \xrightarrow{(180^\circ)xH} \xrightarrow{(90^\circ)xC} -s[yx] \xrightarrow{\delta} \\ -s[yx] \xrightarrow{(180^\circ)xC} s[yx] \xrightarrow{135^\circ yH} 0.7s[yx] \\ +0.7s[yz] \xrightarrow{\delta} \xrightarrow{90^\circ - xC} \xrightarrow{^{1}H-decoupling} 0.7s^2[x1]\end{aligned} \tag{2}$$

2. CH_2 groups

$$[1z1] + [11z] \xrightarrow{\emptyset^\circ yC} \xrightarrow{\delta} \ldots \xrightarrow{\delta} \xrightarrow{90^\circ - xC} 0.35s2^2[x11] - s^4[x11] \tag{3}$$

3. CH_3 groups

$$\begin{aligned}[1z11] + [11z1] + [111z] \xrightarrow{\emptyset^\circ yC} \xrightarrow{\delta} \ldots \xrightarrow{\delta} \xrightarrow{90^\circ - xC} 0.53s2^2c^2[x111] \\ -0.75s2^2s^2[x111] + 1.06s^6[x111]\end{aligned} \tag{4}$$

The final carbon signal intensities, represented by I, for the three groups CH, CH_2 and CH_3 for $\Omega = 90°$ and $\theta = 135°$, as a function of the evolution delay δ and the actual coupling constant J_{CH}, are thus (the operators $[x1]$, $[x11]$, and $[x111]$ have been replaced by the Cartesian operator C_x for simplicity):

$$\begin{aligned}I_{CH} &= C_x\,[0.71 \sin^2(\pi J_{CH}\delta)] \\ I_{CH2} &= C_x\,[0.35 \sin^2(2\pi J_{CH}\delta) - 1.00 \sin^4(\pi J_{CH}\delta)] \\ I_{CH3} &= C_x\,[0.53 \sin^2(2\pi J_{CH}\delta) \cos^2(\pi J_{CH}\delta) - 0.75 \sin^2(2\pi J_{CH}\delta) \sin^2(\pi J_{CH}\delta) + 1.06 \\ &\quad \sin^6(\pi J_{CH}\delta)]\end{aligned} \tag{5}$$

which reduces with $\delta = 1/(2 * {}^{1}J_{CH})$ (matched delay) to:

$$\begin{aligned}I_{CH} &= +0.71\ C_x \\ I_{CH2} &= -1.00\ C_x \\ I_{CH3} &= +1.06\ C_x\end{aligned} \tag{6}$$

Equation (5) provides the analytical expressions to calculate the carbon signal intensities for the three groups CH, CH_2 and CH_3 as a function of the evolution delay δ and the actual coupling constant J_{CH}. Obviously, very weak resonances result in cases of large mismatches between actual $^{1}J_{CH}$ coupling constants and the average $^{1}J_{CH}{}^{0}$ coupling constant set (=1/(2 * δ)) in the DEPTQ experiment. In detail, large mismatches exist (i) for acetylenic CH ($^{1}J_{CH}$ ~ 250 Hz) or hetero aromatic rings ($^{1}J_{CH}$ ~ 170–210 Hz) when $^{1}J_{CH}{}^{0}$ is set to the classical value of 145 Hz, and (ii) for typical methyl groups ($^{1}J_{CH}$ ~ 110–135 Hz) when $^{1}J_{CH}{}^{0}$ is set to an average value 185 Hz, to account for the whole range of $^{1}J_{CH}$ coupling constants (100–250 Hz) when acetylenic CH or hetero aromatic rings are present (Figures S1 and S2).

DEPTQ90, $\Omega = 45°$, $\theta = 90°$

1. CH groups

$$\begin{aligned}[1z] \xrightarrow{\emptyset^\circ yC} \xrightarrow{\delta} \xrightarrow{180^\circ xC} [1z] \xrightarrow{45^\circ xH} -0.7[1y] \xrightarrow{\delta} 0.7s[zx] \xrightarrow{(180^\circ)xH} \xrightarrow{(90^\circ)xC} -0.7s[yx] \xrightarrow{\delta} \\ -0.7s[yx] \xrightarrow{(180^\circ)xC} 0.7s[yx] \xrightarrow{90^\circ yH} -0.7s[yz] \xrightarrow{\delta} \xrightarrow{90^\circ xC} 0.7s^2[x1]\end{aligned} \tag{7}$$

2. CH_2 groups

$$[1z1] + [11z] \xrightarrow{\emptyset°yC} \xrightarrow{\delta} \ldots \xrightarrow{\delta} \xrightarrow{90°-xC} 0.35s2^2[x11] \quad (8)$$

3. CH_3 groups

$$[1z11] + [11z1] + [111z] \xrightarrow{\emptyset°yC} \xrightarrow{\delta} \ldots \xrightarrow{\delta} \xrightarrow{90°-xC} 2.11s^2c^4[x111] \quad (9)$$

The final carbon signal intensities, represented by I, for the three groups CH, CH_2, and CH_3 for $\Omega = 45°$ and $\theta = 90°$, as a function of the evolution delay δ and the actual coupling J_{CH}, are thus:

$$\begin{aligned} I_{CH} &= C_x\,[0.71 \sin^2(\pi J_{CH}\delta)] \\ I_{CH2} &= C_x\,[0.35 \sin^2(2\pi J_{CH}\delta)] \\ I_{CH3} &= C_x\,[2.11 \sin^2(\pi J_{CH}\delta) \cos^4(\pi J_{CH}\delta)] \end{aligned} \quad (10)$$

which reduces with $\delta = 1/(2 * {}^1J_{CH})$ (matched delay) to:

$$\begin{aligned} I_{CH} &= +0.71\ C_x \\ I_{CH2} &= 0 \\ I_{CH3} &= 0 \end{aligned} \quad (11)$$

DEPTQ135_{90} − DEPTQ90_{45}, edited CH_2/CH_3 subspectrum

The subtraction of the two data, DEPTQ135_{90} − DEPTQ90_{45}, leads to:

$$\begin{aligned} I_{CH} &= C_x\,[0.71 \sin^2(\pi J_{CH}\delta)] - C_x\,[0.71 \sin^2(\pi J_{CH}\delta)] = 0 \\ I_{CH2} &= C_x\,[0.35 \sin^2(2\pi J_{CH}\delta) - 1.00 \sin^4(\pi J_{CH}\delta)] - C_x\,[0.35 \sin^2(2\pi J_{CH}\delta)] = -C_x \\ &\sin^4(\pi J_{CH}\delta) \\ I_{CH3} &= C_x\,[0.53 \sin^2(2\pi J_{CH}\delta) \cos^2(\pi J_{CH}\delta) - 0.75 \sin^2(2\pi J_{CH}\delta) \sin^2(\pi J_{CH}\delta) + 1.06 \\ &\sin^6(\pi J_{CH}\delta)] - C_x\,[2.11 \sin^2(\pi J_{CH}\delta) \cos^4(\pi J_{CH}\delta)] \end{aligned} \quad (12)$$

which reduces with $\delta = 1/(2 * {}^1J_{CH})$ (matched delay) to:

$$\begin{aligned} I_{CH2} &= -1.00\ C_x \\ I_{CH3} &= +1.06\ C_x \end{aligned} \quad (13)$$

For the typical J-coupling constant ranges (for which δ is usually set to an average value of 145 Hz), the artefacts originating from CH_2 groups in the DEPTQ90_{45} spectrum are expected to be weak: due to its $\sin^2$-dependence, the intensity of the cross-talk term $0.35 \sin^2(2\pi J_{CH}\delta)$ in Equation (10) is generally small, which is also shown in Figure S3. However, CH_2 artifacts can also be very intense and actually troublesome when the full J-coupling constant range is taken into account (100–250 Hz), for which δ is usually set to a larger average value around 180 Hz (Figure S4) [19,30]. Likewise, for a CH_3 group, the intensity of the cross-talk term $2.11 \sin^2(\pi J_{CH}\delta) \cos^4(\pi J_{CH}\delta)$ in Equation (10) and, thus, CH_3 artifacts, will be very weak for the usual J-coupling constant ranges, as shown in Figure S3, but can also be very intense and troublesome when the full J-coupling constant range is considered (Figure S4) [19,30].

The DEPTQ experiment has two potential drawbacks: (i) the problem of missing or very weak resonances in the DEPTQ135_{90} when large ${}^1J_{CH}$ coupling constant ranges are considered, and (ii) the existence of artefacts, possibly strong, originating from CH_2- and CH_3 groups in the DEPTQ90_{45} spectrum. We propose the modification of the DEPTQ experience to remedy these two weaknesses.

2.1.2. The DEPTQ$^+$ pulse sequence

The proposed DEPTQ$^+$ pulse sequence is depicted in Figure 2 together with the original DEPTQ pulse sequence.[10] Compared to the latter, the evolution periods of length $\delta = 1/(2 * {}^1J_{CH})$ are replaced by three spin echoes of different length [21,30]. Interestingly, these spin-echoes make it possible to omit the first evolution period in the standard DEPTQ pulse sequence that must precede the DEPT pulse sequence for proper refocusing of the Cq-magnetization generated with the first ^{13}C excitation pulse. Therefore, as in the PENDANT sequence [4,5], both the ^{1}H and ^{13}C excitation pulses are synchronized. The total length of DEPTQ$^+$ is, thus, shorter than that of DEPTQ and identical to a standard DEPT experiment, which will reduce the relaxation losses.

The advantages of the DEPTQ$^+$ compared to the DEPTQ experiment, which result from the individual tuning of the three spin echo periods to different $^1J_{CH}$ coupling constants are: (i) a mutual leveling of the DEPT signal intensities, similar to that achieved with the ACCORD-DEPT experiment, which systematically samples a range of $^1J_{CH}$ coupling constants [31]. The accordion principle is, however, more complicated to implement than tuning the three spin echo periods, as shown subsequently. (ii) A reduction in *J* cross-talk in the CH/Cq spectrum (DEPTQ90), although this *J* cross-talk reduction is only noticeable and disturbing for molecules with a large range of $^1J_{CH}$ coupling constants, as shown theoretically (Figures S3 and S4), and subsequently in the experimental part.

Note that the intensities of quaternary carbon resonances are, of course, not affected by these three echo periods used with DEPTQ$^+$ and are the same as with DEPTQ. However, compared to the DEPTQ experiment, note that while the first ^{13}C pulse φ is $\neq 90°$, the additional 180° pulses during the three spin echo periods invert the sign of the residual *z*-magnetization that is not detected. Thus, the phase of the additional 90° ^{13}C pulse prior to data acquisition must be applied along the $+x$ axis to re-establish the residual ^{13}C-z magnetization left with the initial ^{13}C pulse.

Quaternary Carbons

The first ^{13}C pulse ϕ is set arbitrarily (Ernst angle):

$$[z] \xrightarrow{\emptyset°yC} \xrightarrow{\delta_1} \xrightarrow{180°xC} -cos\emptyset[z] + sin\emptyset[x] \xrightarrow{90°xC} cos\emptyset[y] + sin\emptyset[x] \xrightarrow{\delta_2} \xrightarrow{180°xC} \xrightarrow{\delta_3} \xrightarrow{180°xC} cos\emptyset[y] + sin\emptyset[x] \xrightarrow{90°xC} cos\emptyset[z] + sin\emptyset[x] \quad (14)$$

The product operator evaluation for the CH_n coherences originating from initial ^{1}H-polarization is applied in the DEPTQ$^+$ pulse sequence, using the following abbreviations:

$c = \cos(\pi J_{CH}\delta_1)$, $s = \sin(\pi J_{CH}\delta_1)$

$c' = \cos(\pi J_{CH}\delta_2)$, $s' = \sin(\pi J_{CH}\delta_2)$

$c'' = \cos(\pi J_{CH}\delta_3)$, $s'' = \sin(\pi J_{CH}\delta_3)$

$s2'' = \sin(2\pi J_{CH}\delta_3)$

DEPTQ$^+135_{90}$, $\Omega = 90°$, $\theta = 135°$

The final carbon signal intensities, represented by *I*, for the three groups CH, CH_2, and CH_3 for $\Omega = 90°$, $\theta = 135°$, as a function of the evolution delay δ, and the actual coupling constant J_{CH}, are:

1. CH groups

$$[1z] \xrightarrow{90°xH} \xrightarrow{\emptyset°yC} \xrightarrow{\delta_1} \xrightarrow{180°xC} \xrightarrow{180°xH} -[zx] \ldots \xrightarrow{90°xC} -0.71ss''[x1] \quad (15)$$

2. CH_2 groups

$$[1z1] + [11z] \xrightarrow{90°xH} \xrightarrow{90°xH'} \xrightarrow{\emptyset°yC} \xrightarrow{\delta_1} \xrightarrow{180°xC} \xrightarrow{180°xH} \xrightarrow{180°xH'} \ldots \xrightarrow{90°xC} 0.71sc's2''[x11] - ss's''^2[x11] \quad (16)$$

3. CH_3 groups

$$\begin{aligned}&[1z11] + [11z1]\\&+ [111z] \xrightarrow{90°xH} \xrightarrow{90°xH'} \xrightarrow{90°xH''} \xrightarrow{\emptyset°yC} \xrightarrow{\delta_1} \xrightarrow{180°xC} \xrightarrow{180°xH} \xrightarrow{180°xH'} \xrightarrow{180°xH''} \ldots \xrightarrow{90°xC}\\&- 2.11sc'^2s''c''^2[x111] + 3sc's's''^2c''[x111] - 1.06ss'^2s''^3[x111]\end{aligned} \quad (17)$$

The final carbon signal intensities, represented by *I*, for the three groups CH, CH_2, and CH_3 for Ω = 90° and θ = 135°, as a function of the evolution delay δ and the actual coupling constant J_{CH}, are thus:

$$\begin{aligned}&I_{CH} = C_x\,[-0.71\sin(\pi J_{CH}\delta_1)\sin(\pi J_{CH}\delta_3)]\\&I_{CH2} = C_x\,[0.71\sin(\pi J_{CH}\delta_1)\cos(\pi J_{CH}\delta_2)\sin(2\pi J_{CH}\delta_3) - 1.00\sin(\pi J_{CH}\delta_1)\sin(\pi J_{CH}\delta_2)\\&\sin^2(\pi J_{CH}\delta_3)]\\&I_{CH3} = C_x\,[-2.11\sin(\pi J_{CH}\delta_1)\cos^2(\pi J_{CH}\delta_2)\sin(\pi J_{CH}\delta_3)\cos^2(\pi J_{CH}\delta_3) + 3\sin(\pi J_{CH}\delta_1)\\&\cos(\pi J_{CH}\delta_2)\sin(\pi J_{CH}\delta_2)\cos(\pi J_{CH}\delta_3)\sin^2(\pi J_{CH}\delta_3) - 1.06\sin(\pi J_{CH}\delta_1)\sin^2(\pi J_{CH}\delta_2)\\&\sin^3(\pi J_{CH}\delta_3)]\end{aligned} \quad (18)$$

DEPTQ+90_{45}, Ω = 45°, θ= 90°

1. CH groups

$$\begin{aligned}&[1z] \xrightarrow{45°xH} \xrightarrow{\emptyset°yC} \xrightarrow{\delta_1} \xrightarrow{180°xC} \xrightarrow{180°xH} - 0.71s[zx] \xrightarrow{(90°)xC} 0.7s[yx] \xrightarrow{(180°)xH} \xrightarrow{180°xC} \xrightarrow{\delta_2}\\&- 0.71s[yx] \xrightarrow{90°yH} 0.71s[yz] \xrightarrow{(180°)xC} \xrightarrow{(180°)xH} \xrightarrow{\delta} \xrightarrow{90°xC}\\&- 0.71ss''[x1]\end{aligned} \quad (19)$$

2. CH_2 groups

$$[1z1] + [11z] \xrightarrow{45°xH} \xrightarrow{\emptyset°yC} \xrightarrow{\delta_1} \xrightarrow{180°xC} \xrightarrow{180°xH} \xrightarrow{180°xH'} \ldots \xrightarrow{\delta} \xrightarrow{90°xC} - 0.71sc's2''[x11 \quad (20)$$

3. CH_3 groups

$$\begin{aligned}&[1z11] + [11z1] + [111z] \xrightarrow{45°xH} \xrightarrow{\emptyset°yC} \xrightarrow{\delta_1} \xrightarrow{180°xC} \xrightarrow{180°xH} \xrightarrow{180°xH'} \ldots \xrightarrow{\delta} \xrightarrow{90°xC}\\&- 2.11sc'^2s''c''^2[x111]\end{aligned} \quad (21)$$

The final carbon signal intensities, represented by *I*, for the three groups CH, CH_2, and CH_3 for Ω = 45° and θ = 90°, as a function of the three evolution delays δ_1, δ_2 and δ_3 and the actual coupling J_{CH}, are therefore:

$$\begin{aligned}&I_{CH} = -C_x\,[0.71\sin(\pi J_{CH}\delta_1)\sin(\pi J_{CH}\delta_3)]\\&I_{CH2} = -C_x\,[0.71\sin(\pi J_{CH}\delta_1)\cos(\pi J_{CH}\delta_2)\sin(2\pi J_{CH}\delta_3)]\\&I_{CH3} = -C_x\,[2.11\sin(\pi J_{CH}\delta_1)\cos^2(\pi J_{CH}\delta_2)\sin(\pi J_{CH}\delta_3)\cos^2(\pi J_{CH}\delta_3)]\end{aligned} \quad (22)$$

For the DEPTQ and DEPTQ+ experiments, the approximate carbon signal intensities, represented by *I* (for $^1J_{CH} \approx {}^1J_{CH}{}^0$), for the three groups CH, CH_2, and CH_3 for Ω = 90° and θ = 135°, as a function of the coupling constant $^1J_{CH}$ and δ, δ_1, δ_2, and δ_3, are summarized in Table 1:

Table 1. Final carbon signal intensities, represented by *I*, for the three groups CH, CH_2, and CH_3 for Ω = 90°, θ = 135°, as a function of the coupling constant J_{CH} and the delays δ, δ_1, δ_2, and δ_3.

	DEPTQ	**DEPTQ+**
CH groups	$0.71C_x\sin^2(\pi J_{CH}\delta)$	$-0.71C_x\sin(\pi J_{CH}\delta_1)\sin(\pi J_{CH}\delta_3)$
CH_2 groups	$-C_x\sin^4(\pi J_{CH}\delta)$	$-C_x\sin(\pi J_{CH}\delta_1)\sin(\pi J_{CH}\delta_2)\sin^2(\pi J_{CH}\delta_3)$

CH_3 groups	$1.06C_x\sin^6(\pi J_{CH}\delta)$	$-1.06C_x\sin(\pi J_{CH}\delta_1)\sin^2(\pi J_{CH}\delta_2)\sin^3(\pi J_{CH}\delta_3)$

According to the above relations for Ω = 90° and θ = 135° and compared to the DEPTQ experiment, the signs of the signal intensities for CH and CH_3 groups are *inverted* using the DEPTQ$^+$ experiment, while the sign of the signal intensities for CH_2 groups is *identical*. Consequently, the usual angle θ for achieving the DEPT editing, CH/CH_3 positive, CH_2 negative, is obtained for θ = 45° and not for θ = 135°, as would be valid for DEPTQ (Table 2).

Table 2. DEPTQ and DEPTQ$^+$: maximal amplitude of CH, CH_2, and CH_3 groups for the three usual angles θ and for Ω = 90°

Experiment	Angle θ	Amplitude of CH	Amplitude of CH_2	Amplitude of CH_3
DEPTQ$^+$	45°	−0.71	1	−1.06
DEPTQ		0.71	1	1.06
DEPTQ$^+$	90°	−1	0	0
DEPTQ		1	0	0
DEPTQ$^+$	135°	−0.71	−1	−1.06
DEPTQ		0.71	−1	1.06

To separate the signals of CH, C_q and CH_2, CH_3 groups in different sub-spectra and to obtain different signs for the signals of CH_2 and CH_3 groups the first adjustable proton pulse Ω and the editing pulse θ must therefore be set for the DEPTQ$^+$ experiment to 45° and 90° (DEPTQ$^+$$90_{45}$) and to 90° and 45°, respectively (DEPTQ$^+$$45_{90}$). Subtracting the DEPTQ$^+$$90_{45}$ spectrum, showing exclusively the Cq and CH signals with opposite phases, from the DEPTQ$^+$$45_{90}$ spectrum results in a CH_2/CH_3 edited spectrum with the signals of the two carbon types with opposite phases.

Interestingly, equations 15–22 show that the intensities of the signals of the three carbon types depend differently and for CH *solely* on *two* (δ_1 and δ_3) of the individual delays δ_1, δ_2, and δ_3, which is the basis for efficiently leveling the signal intensities for all multiplicities with the DEPTQ$^+$ pulse sequence, even for large $^1J_{CH}$ coupling constant ranges. Indeed, and with the specific ranges of $^1J_{CH}$-coupling constants for the three carbon types, i.e., CH: [120 < $^1J_{CH}$ < 250 Hz], CH_2: [115 < $^1J_{CH}$< 175 Hz], CH_3: [100 < $^1J_{CH}$< 135 Hz], the three delays δ_1, δ_2, and δ_3 can be individually and optimally adjusted. For instance, δ_2 which does not affect CH-intensities can be adjusted for small $^1J_{CH}$ coupling constants, typically 120 Hz, to maximize the signals of CH_2 and CH_3 groups. On the other hand, δ_1 can be adjusted for large $^1J_{CH}$ coupling constants, typically 220–230 Hz, to maximize the signals of acetylenic CH groups. Finally, δ_3 can be adjusted for an average $^1J_{CH}$ coupling constant, typically 185 Hz, to account for all carbon types present. This enables real leveling of the signal intensities with the DEPTQ$^+$ experiment, as demonstrated theoretically (Figures S3–S5), and, in the following section, practically.

2.2. Experimental Results

2.2.1. Cholesteryl Acetate

We first used a sample of 100 mmol cholesteryl acetate (Figure 3, 30 mg dissolved in 0.7 mL $CDCl_3$) for testing the performance of the DEPTQ$^+$ experiment.

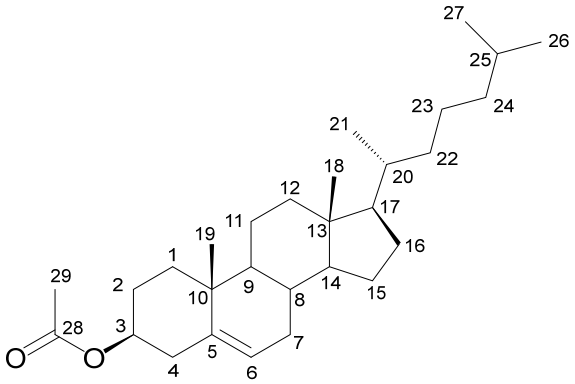

Figure 3. Cholesteryl acetate and carbon numbering.

In Figures 4 and 5, the DEPTQ135$_{90}$, DEPTQ90$_{45}$, the difference between DEPTQ135$_{90}$ and DEPTQ90$_{45}$ (Figure 4), the DEPTQ^{+}45$_{90}$, DEPTQ^{+}90$_{45}$, and the difference between DEPTQ^{+}45$_{90}$ and DEPTQ^{+}90$_{45}$ (Figure 5) of cholesteryl acetate are shown. Cholesteryl acetate (Figure 3) is a molecule exhibiting a narrow range of coupling constants $^{1}J_{CH}$ (122 Hz for $^{1}J_{C26H26}$ to 155 Hz for $^{1}J_{C6H6}$). Accordingly, both the DEPTQ90$_{45}$ providing a Cq/CH edited spectrum and the DEPTQ90$_{45}$ providing a CH_2/CH_3 edited spectrum (difference between DEPTQ135$_{90}$ and DEPTQ90$_{45}$) are of high quality, with few and weak CH_2/CH_3 artefacts in the DEPTQ90$_{45}$ and some residual CH peaks in the difference spectrum, respectively (Figure 4).

The same, nearly identical results have been obtained using the proposed DEPTQ^{+} pulse sequence. Thus, the DEPTQ^{+} behaves similarly to the DEPTQ experiment if the narrow, usual range of coupling constants $^{1}J_{CH}$ is present: the mutual signal intensity leveling and the *J* cross-talk reduction only provide very minor improvements.

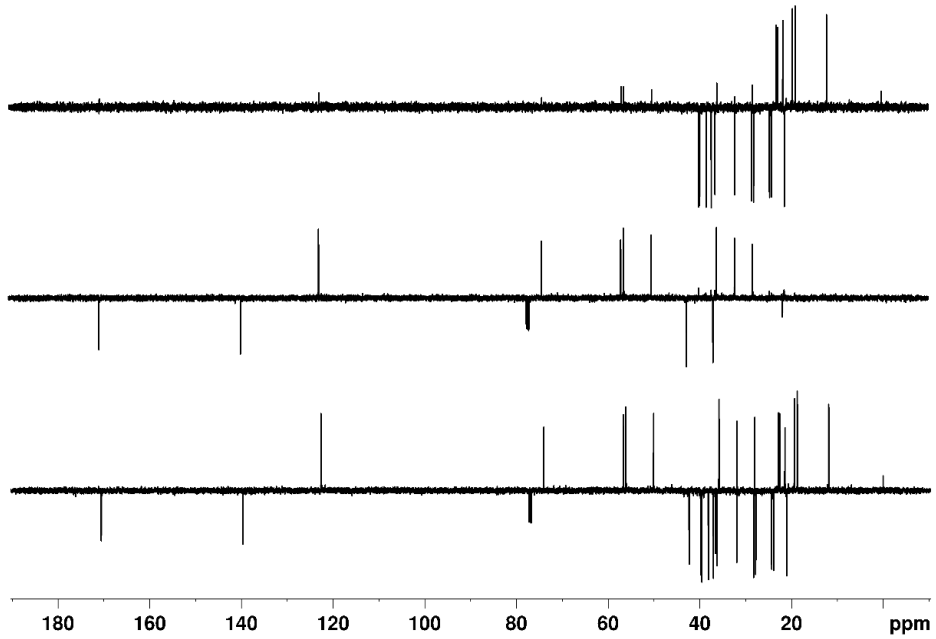

Figure 4. Bottom: DEPTQ135$_{90}$; **middle**: DEPTQ90$_{45}$; **top**: Difference between DEPTQ135$_{90}$ and DEPTQ90$_{45}$ spectra of 30 mg of cholesteryl acetate dissolved in 0.7 mL $CDCl_3$. The delay δ was set to 3.45 ms, adjusted for a coupling constant $^{1}J_{CH}$ of 145 Hz.

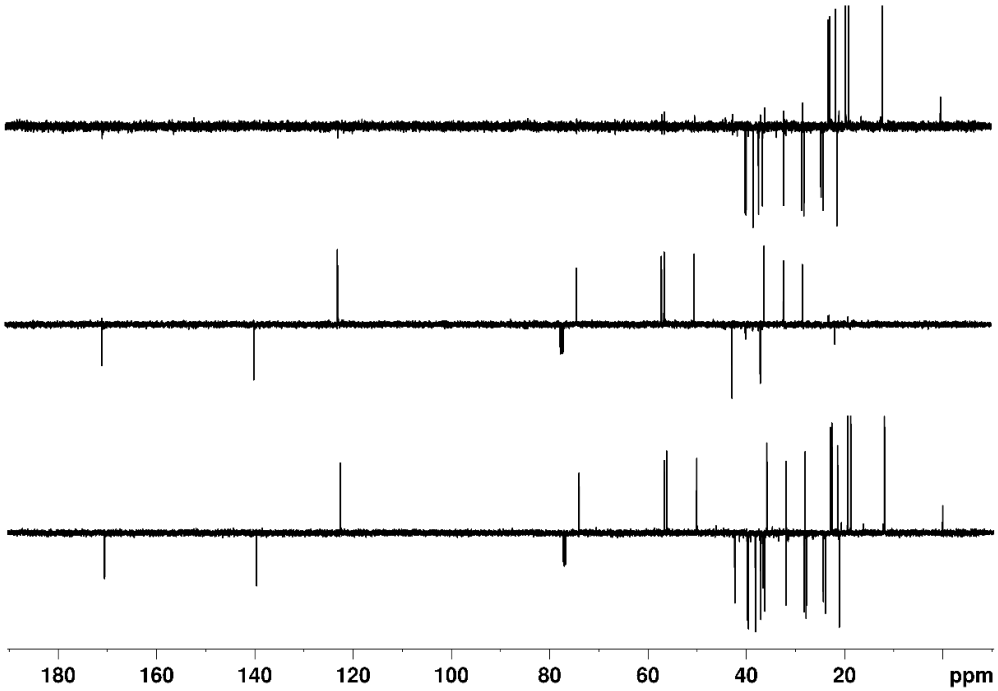

Figure 5. Bottom: DEPTQ$^{+}45_{90}$; **middle**: DEPTQ$^{+}90_{45}$; **top**: Difference between DEPTQ$^{+}45_{90}$ and DEPTQ$^{+}90_{45}$ spectra of 30 mg of cholesteryl acetate dissolved in 0.7 mL $CDCl_3$. The delays δ_1, δ_2, and δ_3 were set to 3.13 ms, adjusted for a coupling constant $^1J_{CH}$ of 160 Hz, to 4.35 ms, adjusted for a coupling constant $^1J_{CH}$ of 115 Hz, and to 3.45 ms, adjusted for a coupling constant $^1J_{CH}$ of 145 Hz, respectively.

However, the superiority of the DEPTQ^{+} experiment becomes clear when there is a larger range of coupling constants $^1J_{CH}$. First, with the sole aim of demonstrating the potential and performance of the DEPTQ^{+} experiment, we used the same molecule of cholesteryl acetate but adjusted the three delays in the experiments as if all $^1J_{CH}$ coupling constants (alkanes, aromatics, alkynes) were present. The spectra are shown in Figures S8 and S9.

In this case, it is clear that the DEPTQ^{+} behaves much better than the DEPTQ experiment; even the standard DEPTQ135 spectrum is confusing, since the resonances of the methyl groups between 10 and 30 ppm are barely visible (Figure S8), as predicted theoretically (Figure S2). This is due to the very large mismatch between the actual $^1J_{CH}$ coupling constants in methyl groups (~125 Hz) and the average $^1J_{CH}{}^0$ coupling constant set in the DEPTQ experiment, $^1J_{CH}{}^0$ = 185 Hz, intentionally set to cover the whole range of $^1J_{CH}$ coupling constants (100–250 Hz). The DEPTQ90_{45} is also confusing, with many residual CH_2/CH_3 signals present, which makes the identification of CH groups difficult, as they are as intense (strong *J* cross talk) and have the same sign as the CH signals (Figure S8). Finally, the "CH_2/CH_3" edited spectrum (difference between DEPTQ135_{90} and DEPTQ90_{45}) is extremely confusing, as only the resonances of CH_2 groups are present, while the resonances of CH_3 groups are either barely visible or even completely absent (Figure S8).

In contrast, the spectra obtained using the DEPTQ^{+} pulse sequence are much better and sufficient for reliable identification of CH_n groups: In the DEPTQ$^{+}45_{90}$ spectrum, the resonances of the methyl groups between 10 and 30 ppm are clearly visible and intense (Figure S9), as predicted theoretically (Figure S7). This is because the three delays δ_1, δ_2, and δ_3 in the DEPTQ^{+} experiment are matched to three different $^1J_{CH}{}^0$ coupling constants (230, 125, 165 Hz, respectively), which results in a mutual leveling of the DEPT signal intensities. In the DEPTQ$^{+}90_{45}$, there are only very few and weak CH_2/CH_3 artefacts (weak

J cross talk), which enables easy identification of CH groups (Figure S9). Finally, the "CH_2/CH_3" edited spectrum also allows a reliable identification of the clearly visible resonances of CH_2 groups and of CH_3 (Figure S9).

2.2.2. 4-methyl-*N*,*N*-di(prop-2-yn-1-yl)aniline

In order to test the effective performance, we finally tried the DEPTQ$^+$ experiment on the demanding sample of ~30 mg of 4-methyl-*N*,*N*-di(prop-2-yn-1-yl)aniline dissolved in 0.7 mL $CDCl_3$ (Figure 1). 4-methyl-*N*,*N*-di(prop-2-yn-1-yl)aniline contains alkane, aromatic and alkyne groups with the full range of $^1J_{CH}$ coupling constants (125 Hz for $^1J_{C8H8}$ to 248 Hz for $^1J_{C1H1}$). Note also the very particular case of C2 at 79.4 ppm, which, with its large long-range coupling ($^2J_{C2H1}$ ~ 50 Hz), behaves like a pseudo- or only partially quaternary carbon.

In Figures 6 and 7, the DEPTQ135$_{90}$, DEPTQ90$_{45}$, the difference between DEPTQ135$_{90}$ and DEPTQ90$_{45}$ (Figure 6), and the DEPTQ$^+$45$_{90}$, DEPTQ$^+$90$_{45}$, and the difference between DEPTQ$^+$45$_{90}$ and DEPTQ$^+$90$_{45}$ (Figure 7) of 4-methyl-*N*,*N*-di(prop-2-yn-1-yl)aniline are shown.

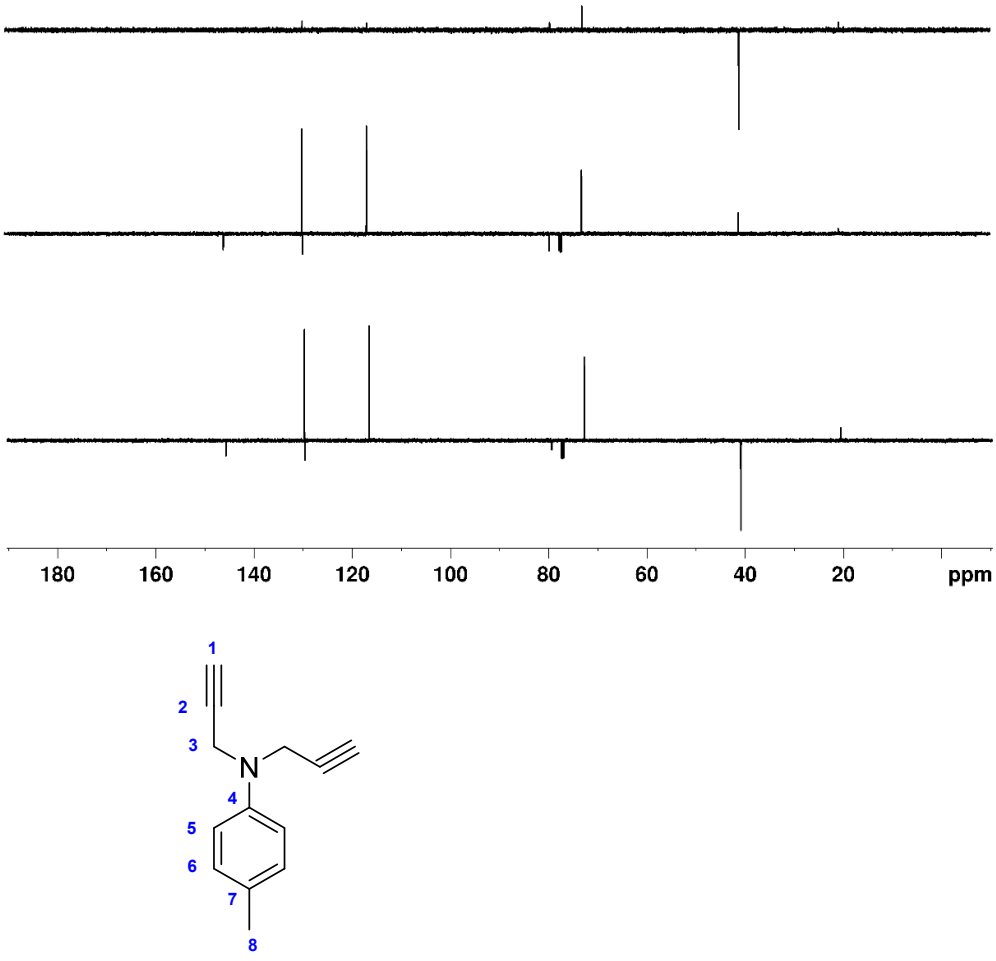

Figure 6. Bottom: DEPTQ135$_{90}$, **middle**: DEPTQ90$_{45}$; **top**: Difference between DEPTQ135$_{90}$ and DEPTQ90$_{45}$ spectra of ~30 mg of 4-methyl-*N*,*N*-di(prop-2-yn-1-yl)aniline dissolved in 0.7 mL $CDCl_3$. The delay δ was set to 2.70 ms, adjusted for a coupling constant $^1J_{CH}$ of 185 Hz. The relaxation delay was 4 s, the NOE building period 3 s. All other parameters are identical to those described in the Materials and Methods section. The structure of 4-methyl-*N*,*N*-di(prop-2-yn-1-yl)aniline and carbon numbering is shown below the spectra.

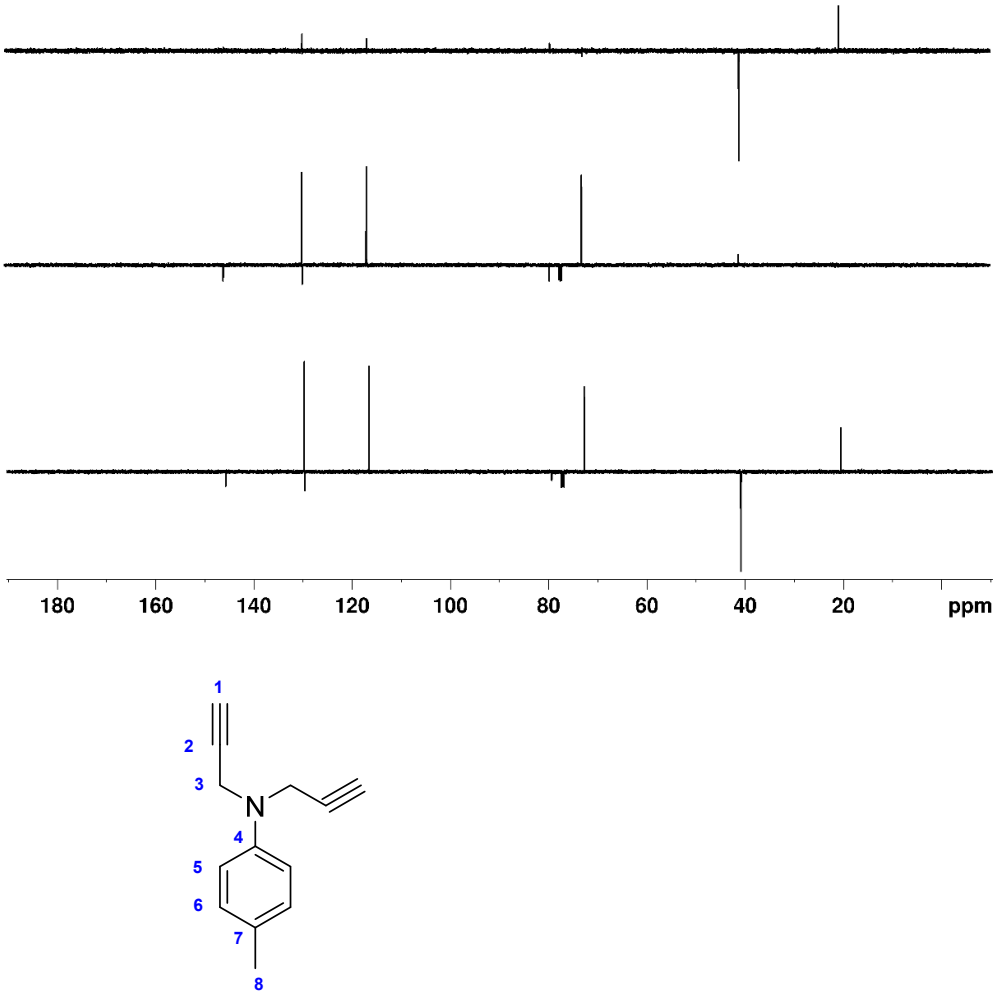

Figure 7. Bottom: DEPTQ$^{+}45_{90}$; **middle**: DEPTQ$^{+}90_{45}$; **top**: Difference between DEPTQ$^{+}45_{90}$ and DEPTQ$^{+}90_{45}$ spectra of ~30 mg of 4-methyl-*N*,*N*-di(prop-2-yn-1-yl)aniline dissolved in 0.7 mL $CDCl_3$. The delays δ_1, δ_2, and δ_3 were set to 2.18 ms, adjusted for a coupling constant $^1J_{CH}$ of 230 Hz, to 4.00 ms, adjusted for a coupling constant $^1J_{CH}$ of 125 Hz, and to 3.18 ms, adjusted for a coupling constant $^1J_{CH}$ of 165 Hz, respectively. The relaxation delay was 4 s, the NOE building period 3s. All other parameters are identical to those described in the Materials and Methods section. The structure of 4-methyl-*N*,*N*-di(prop-2-yn-1-yl)aniline and carbon numbering is shown below the spectra.

With 4-methyl-*N*,*N*-di(prop-2-yn-1-yl)aniline, it is clear that the DEPTQ^{+} performs much better than the DEPTQ experiment: the standard DEPTQ135 spectrum is useable, but the resonance of the methyl group C8 at 20.6 ppm is very weak (Figure 6). As already mentioned, this is due to the very large mismatch between the actual $^1J_{CH}$ coupling constants in methyl groups (~125 Hz) and the large average $^1J_{CH}{}^0$ coupling constant set in the DEPTQ experiment, $^1J_{CH}{}^0$ = 185 Hz (Figure S2). Artefacts (*J* cross talk) belonging to the CH_2 C3 at 40.9 ppm and to the CH_3 C8 at 20.6 ppm are visible in the DEPTQ90_{45}, even if their intensities are rather small (Figure 6). Such artefacts can be problematic with unknown molecular structures or if the attribution is performed in an automatic or semi-automatic way using dedicated attribution software. Particularly confusing is the "CH_2/CH_3" edited spectrum obtained with DEPTQ (difference between DEPTQ135_{90} and DEPTQ90_{45}), with a strong signal of the CH_2 groups C3 at 40.9 ppm and a weak residual signal of the CH group C1, while the resonance of the CH_3 group C8 at 20.6 ppm is almost invisible (Figure 6). In addition, the residual signal of C1 at 72.8 ppm could be misleading or misinterpreted by attribution/analysis software.

In contrast, the spectra obtained using the DEPTQ$^+$ pulse sequence are less confusing and sufficient for reliable carbon type identification: in the DEPTQ$^+45_{90}$, the resonance of the methyl group C8 around 20 ppm is clearly visible and intense (Figure 7). This must be attributed to the individual tuning of the *three* delays to different $^1J_{CH}{}^0$ coupling constants (125, 175, 230 Hz), which results in a mutual leveling of the DEPT signal intensities. The DEPTQ$^+90_{45}$ shows—besides the negative quaternary carbon signals—the three strong CH signals with only one weak CH_2 artifact (weak *J* cross talk) present (Figure 7). Finally, the CH_2/CH_3 edited spectrum is almost perfect, with the strong resonances of the CH_2- and CH_3 groups C3 and C8 in anti-phase and only very weak residual signals left (Figure 7).

2.3. Practical Aspects

Our theoretical and practical investigations show that the proposed new DEPTQ$^+45_{90}$ and DEPTQ$^+90_{45}$ experiments work well. However, the experimental results suggest that the quality of spectral editing also depends on the relaxation delay. While for medium sized molecules such as cholesteryl acetate, the length of the relaxation delay affects only the intensity of the slow relaxing carbons but not the editing quality (Figure S10), it becomes critical also for the editing procedure for small molecules and/or groups exhibiting long T_1 relaxation times.

This manifests itself with 4-methyl-*N*,*N*-di(prop-2-yn-1-yl)aniline, for which the intensities of the CH signals in the DEPTQ$^+90_{45}$ spectra can be drastically different to that obtained in the DEPTQ$^+45_{90}$ if overly short relaxation delays are used. The numerous and intense "CH-artefacts" showing up in the edited CH_2/CH_3 spectrum may be potentially attributed to CH_3 groups. The influence of relaxation and the need for choosing the relaxation delay(s) long enough with DETPQ$^+$ to achieve a sufficient editing quality are corroborated by simulated spectra, which are in good agreement with the corresponding experimental spectra shown in Figures S11 and S12.

Finally, we wish to concentrate on the overall sensitivities of DEPTQ$^+$, and to compare it with DEPTQ and the usually performed "tandem alternatives" such as ^{13}C one-pulse/DEPT. In previous reports [9–11], Bigler et al. have compared spectra acquired DEPTQ and the ^{13}C one-pulse spectra with an equal number of scans within the same total measuring time, and found that the DEPTQ spectrum decreases signal intensities of quaternary carbons by 15% and 10% when compared to the ^{13}C one-pulse. The corresponding experiments (DEPTQ vs. ^{13}C one-pulse + DEPT) based on equal total measuring times showed average S/N ratios of about 70% and 85% for the CH_n signals in the DEPT spectrum, compared to the corresponding values of the DEPTQ experiment [10]. While the signal intensities of quaternary carbons are identical in DEPTQ and DEPTQ$^+$ spectra, the comparison of the average S/N ratio for the CH_n signals between DEPTQ and DEPTQ$^+$ is not so straightforward. While for standard DEPTQ experiments, as shown in this manuscript, the signals at the extremes of the $^1J_{CH}$ coupling range suffer in intensity or cannot be detected, DEPTQ$^+$ experiments (similar to ACCORD-DEPT experiments [31]) provide spectra with notably improved S/N ratios for these specific signals. However, owing to the mutual signal intensity leveling, DEPTQ$^+$ always provides either better or worse signal intensity compared to standard optimization. The S/N ratio for some signals will correspondingly decrease compared to a standard optimized DEPTQ experiment.

3. Materials and Methods

3.1. Synthesis and Characterization of 4-Methyl-N,N-di(prop-2-yn-1-yl)aniline

The chemicals were purchased from Aldrich, Alfa Aesar, Acros Organics, and TCI Chemicals and used without further purification, In a flame-dried round bottom flask equipped with a magnetic stirrer, *p*-toluidine (0.5 g, 4.6 mmol) and anhydrous K_2CO_3 (0.77 g, 5.52 mmol) were mixed in dry dimethylformamide (10 mL). Propargyl bromide (0.65 g, 5.52 mmol) was then added dropwise during a period of 15 min and the resulting mixture

was stirred under nitrogen atmosphere for 5 h. After completion of the reaction (monitored by TLC), the mixture was poured into water (10 mL) and extracted with ethyl acetate (2 × 15 mL). The combined organic layers were washed with water (4 × 10 mL) and brine (10 mL), dried over sodium sulfate, filtered, and concentrated under reduced pressure.[32,33] The reaction crude was purified by column chromatography (Silica, 230–400 mesh) using mixtures of hexane/ethyl acetate (30:1). The desired product was obtained as a highly dense yellow oil (110 mg, 13%) along with the product of mono substitution 4-methyl-*N*-(prop-2-yn-1-yl)aniline (500 mg, 75%).

4-methyl-N,N-di(prop-2-yn-1-yl)aniline: ^{1}H NMR (300 MHz, $CDCl_3$) δ 7.12 (d, *J* = 8.6 Hz, 2H), 6.92 (d, *J* = 8.6 Hz, 2H), 4.11 (d, *J* = 2.4 Hz, 4H), 2.30 (s, 3H), 2.26 (t, *J* = 2.4 Hz, 2H). ^{13}C NMR (75 MHz, $CDCl_3$) δ 145.8 (C4), 129.8 (C5), 129.7 (C7), 116.7 (C6), 79.4 (C2), 72.8 (C1), 40.9 (C3), 20.6 (C8). The spectra are referenced with respect to the residual $CHCl_3$ resonance (7.264 ppm) and to the ^{13}C resonance of $CDCl_3$ (77.16 ppm).

3.2. NMR Measurements

All DEPTQ and DEPTQ^{+} experiments were recorded on a Bruker AvanceII 500 MHz NMR spectrometer equipped with a 5 mm BBI Inverse probehead. The samples used were: (i) the standard test sample provided with Bruker NMR spectrometers, 30 mg of cholesteryl acetate dissolved in 0.7 mL $CDCl_3$, and (ii) ~30 mg of 4-methyl-*N,N*-di(prop-2-yn-1-yl)aniline dissolved in 0.7 mL $CDCl_3$. ^{1}H and ^{13}C 90° pulse lengths were 8.4 μs and 13.2 μs, respectively. The composite chirp pulse for refocusing has a duration of 2 ms, is defined by 4000 points and by 20% smoothing and 60 kHz sweep width (Crp60comp.4 in the Bruker wave form library). The experimental details of the measurements are as follows. Cholesteryl acetate: if not otherwise mentioned, all spectra were acquired with 128 k real data points with a relaxation delay of 4 s, a NOE building period of 3 s, 64 scans for a total experimental time of approximately 7 min. ^{13}C spectral widths were 200 ppm, leading to an acquisition time of 2.60 s. Data were processed with 128 k data points using exponential multiplication with a line broadening of 1 Hz. 4-methyl-*N,N*-di(prop-2-yn-1-yl)aniline: the spectra were acquired with 128 k data points with a relaxation delay of 10 s, a NOE building period of 5 s, 16 scans for a total experimental time of approximately 3 min. ^{13}C spectral widths were 200 ppm, leading to an acquisition time of 2.60 s. Data were processed with 128 k data points using exponential multiplication with a line broadening of 1 Hz.

3.3. Numerical Simulations

The numerical simulations shown in Figures S1–S7 have been performed with Microsoft Excel®, Office 365 for Windows. Relaxation effects during both pulse sequences were not considered.

3.4. NMR Simulations

The simulations shown in Figures S10 and S11 have been performed with the BRUKER NMRSIM program for MAC (version 5.5.3. 2012). The simulated DEPTQ and DEPTQ^{+} spectra are obtained for 4-methyl-*N,N*-di(prop-2-yn-1-yl)aniline. The parameters used for the simulations were: $^{1}J_{C1H1}$ = 260 Hz, $^{1}J_{C3H3}$ = 145 Hz, $^{1}J_{C5H5}$ = $^{1}J_{C6H6}$ = 165 Hz, $^{1}J_{C8H8}$ = 125 Hz, $^{2}J_{C2H1}$ = 50 Hz. The relaxation times have been set to T_1 = 1 s for all CH_n groups, and T_1 = 5 s for the quaternary carbons, T_2 = 0.5 s, and full relaxation during both the pulse sequence and final data acquisition were considered. The chemical shifts set in the simulations were the experimental chemical shifts.

4. Conclusions

Compared to the DEPTQ experiment, the proposed new DEPTQ^{+} experiment is shorter and the different evolution delays are designed as spin echoes, which can be matched to different $^{1}J_{CH}$ values. We have shown, both theoretically and experimentally,

that for molecules with a standard range of $^1J_{CH}$ coupling constants (i.e., 110180 Hz), the differences between DEPTQ and DEPTQ$^+$ are minimal. The differences become appreciable for molecules possessing a large range of $^1J_{CH}$ coupling constants. The DEPTQ$^+$ experiment makes it possible to obtain DEPTQ spectra with (i) a mutual leveling of the DEPT signal intensities, (ii) a reduction in *J* cross-talk in the Cq/CH spectrum, and (iii) more reliable CH_2/CH_3 edited spectra.

The influence of relaxation and the need to choose a relaxation delay that is sufficiently long, with DETPQ$^+$, to obtain reliable data and clean edited spectra represents the only limitation of this study, but this is valid for molecules with long T_1 relaxation times. This is, however, also the case with the original DEPTQ experiment.

In conclusion, the new DEPTQ$^+$ experiment is expected to be attractive for fast ^{13}C analysis of small-to medium sized molecules, especially those with a large range of $^1J_{CH}$ coupling constant, and especially in high-throughput laboratories. With concentrated samples and/or by exploiting the high sensitivity of cryogenically cooled ^{13}C NMR probeheads, the efficacy of such investigations may be improved, as it is possible to unequivocally identify all carbon multiplicities with only one scan for each of the two independent DEPTQ$^+$ experiments.

Supplementary Materials: The following are available online. Figure S1: DEPTQ135$_{90}$: theoretical amplitude of a CH group as a function of the $^1J_{CH}$ coupling constant, Figure S2: DEPTQ135$_{90}$: theoretical amplitude of CH_3 groups as a function of the $^1J_{CH}$ coupling constant, Figure S3: DEPTQ90$_{45}$ and DEPTQ$^+$90$_{45}$: theoretical residual amplitude of CH_2 and CH_3 groups, usual $^1J_{CH}$ coupling constant range, Figure S4: DEPTQ90$_{45}$ and DEPTQ$^+$90$_{45}$: theoretical residual amplitude of CH_2 and CH_3 groups, full $^1J_{CH}$ coupling constant range, Figure S5: DEPTQ90$_{45}$ and DEPTQ$^+$90$_{45}$: theoretical amplitude of CH groups, full $^1J_{CH}$ coupling constant range, Figure S6: DEPTQ90$_{45}$ and DEPTQ$^+$90$_{45}$: theoretical amplitude of CH_2 groups, full $^1J_{CH}$ coupling constant range, Figure S7: DEPTQ90$_{45}$ and DEPTQ$^+$90$_{45}$: theoretical amplitude of CH_3 groups, full $^1J_{CH}$ coupling constant range, Figure S8: DEPTQ135$_{90}$, DEPTQ90$_{45}$ and (CH_2/CH_3) edited spectra of cholesteryl acetate, adjusted for a coupling constant $^1J_{CH}$ of 185 Hz, Figure S9: DEPTQ$^+$45$_{90}$, DEPTQ$^+$90$_{45}$ and (CH_2/CH_3) edited spectra of cholesteryl acetate, Figure S10: DEPTQ and DEPTQ$^+$ spectra of cholesteryl acetate: influence of the relaxation delay, Figure S11: Theoretical and DEPTQ and DEPTQ$^+$ spectra of 4-methyl-*N*,*N*-di(prop-2-yn-1-yl)aniline: relaxation delay = 2s, Figure S12: Theoretical and DEPTQ and DEPTQ$^+$ spectra of 4-methyl-*N*,*N*-di(prop-2-yn-1-yl)aniline: relaxation delay = 20s.

Author Contributions: Conceptualization, P.B. and J.F.; methodology, P.B., C.M. and J.F.; software, P.B. and J.F.; validation, P.B. and J.F.; formal analysis, P.B. and J.F.; investigation, P.B. and J.F.; resources, J.F.; data curation, P.B. and J.F.; writing—original draft preparation, P.B., C.M. and J.F.; writing—review and editing, P.B. and J.F.; visualization, P.B. and J.F.; supervision, P.B. and J.F.; project administration, J.F.; funding acquisition, J.F. All authors have read and agreed to the published version of the manuscript.

Funding: This research and the APC were funded by the University of Berne.

Institutional Review Board Statement Not applicable.

Informed Consent Statement: Not applicable.

Conflicts of Interest: The authors declare no conflict of interest.

Sample Availability: Samples of the compound 4-methyl-*N*,*N*-di(prop-2-yn-1-yl)aniline are available from the authors. Cholesteryl acetate is commercially available.

References

1. Saurí, J.; Liu, Y.; Parella, T.; Williamson, R.T.; Martin, G.E. Selecting the Most Appropriate NMR Experiment to Access Weak and/or Very Long-Range Heteronuclear Correlations. *J. Nat. Prod.* **2016**, *79*, 1400–1406, doi:10.1021/acs.jnatprod.6b00139.
2. Le Cocq, C.; Lallemand, J.-Y. Precise carbon-13 n.m.r. multiplicity determination. *J. Chem. Soc. Chem. Commun.* **1981**, 150–152, doi:10.1039/c39810000150.
3. Patt, S.L.; Shoorley, J.N. Attached Proton Test for Carbon-13 NMR. *J. Magn. Reson.* **1982**, *46*, 535–539.
4. Homer, J.; Perry, M.C. New method for NMR signal enhancement by polarization transfer, and attached nucleus testing. *J. Chem. Soc. Chem. Commun.* **1994**, 373–374, doi:10.1039/c39940000373.

5. Homer, J.; Perry, M.C. Enhancement of the NMR spectra of insensitive nuclei using PENDANT with long-range coupling constants. *J. Chem. Soc. Perkin Trans. 2* **1995**, 533–536, doi:10.1039/p29950000533.
6. Burum, D.; Ernst, R. Net polarization transfer via a J-ordered state for signal enhancement of low-sensitivity nuclei. *J. Magn. Reson.* **1980**, *39*, 163–168, doi:10.1016/0022-2364(80)90168-7.
7. Dodrell, D.M.; Pegg, D.T.; Bendall, M.R. Distortionless enhancement of NMR signals by polarization transfer. *J. Magn. Reson.* **1982**, *48*, 323–327.
8. Primasova, H.; Bigler, P.; Furrer, J. Chapter One—The DEPT Experiment and Some of Its Useful Variants. In *Annual Reports on NMR Spectroscopy*; Webb, G.A., Ed.; Academic Press: Cambridge, MA, USA, 2017; Volume 92, pp. 1–82.
9. Burger, R.; Bigler, P. DEPTQ: Distortionless enhancement by polarization transfer including the detection of quaternary nuclei. *J. Magn. Reson.* **1998**, *135*, 529–534.
10. Bigler, P.; Kümmerle, R.; Bermel, W. Multiplicity editing including quaternary carbons: Improved performance for the13C-DEPTQ pulse sequence. *Magn. Reson. Chem.* **2007**, *45*, 469–472, doi:10.1002/mrc.1993.
11. Bigler, P. Fast 13 C-NMR Spectral Editing for Determining CH n Multiplicities. *Spectrosc. Lett.* **2008**, *41*, 162–165, doi:10.1080/00387010802008005.
12. Bildsøe, H.; Dønstrup, S.; Jakobsen, H.; Sørensen, O. Subspectral editing using a multiple quantum trap: Analysis of J cross-talk. *J. Magn. Reson.* **1983**, *53*, 154–162, doi:10.1016/0022-2364(83)90087-2.
13. Furrer, J. Old and new experiments for obtaining quaternary-carbon-only NMR spectra. *Appl. Spectrosc. Rev.* **2021**, *56*, 128–142, doi:10.1080/05704928.2020.1756838.
14. Bodenhausen, G.; Ruben, D.J. Natural abundance nitrogen-15 NMR by enhanced heteronuclear spectroscopy. *Chem. Phys. Lett.* **1980**, *69*, 185–189, doi:10.1016/0009-2614(80)80041-8.
15. Bax, A.; Subramanian, S. Sensitivity-enhanced two-dimensional heteronuclear shift correla-tion NMR spectroscopy. *J. Magn. Reson.* **1986**, *67*, 565–569.
16. Furrer, J. A comprehensive discussion of hmbc pulse sequences, part 1: The classical HMBC. *Concepts Magn. Reson. Part. A* **2012**, *40*, 101–127, doi:10.1002/cmr.a.21232.
17. Reynolds, W.F.; Burns, D.C. Getting the Most Out of HSQC and HMBC Spectra. In *Annual Reports on NMR Spectroscopy*; Webb, G.A., Ed.; Annual Reports on NMR Spectroscopy; Elsevier BV: Amsterdam, The Netherlands, 2012; Volume 76, pp. 1–21.
18. Williamson, R.T.; Buevich, A.V.; Martin, G.E.; Parella, T. LR-HSQMBC: A Sensitive NMR Technique to Probe Very Long-Range Heteronuclear Coupling Pathways. *J. Org. Chem.* **2014**, *79*, 3887–3894, doi:10.1021/jo500333u.
19. Furrer, J. A comprehensive discussion of HMBC pulse sequences. 2. Some useful variants. *Concepts Magn. Reson. Part. A* **2012**, *40*, 146–169, doi:10.1002/cmr.a.21231.
20. Saurí, J.; Frédérich, M.; Tchinda, A.T.; Parella, T.; Williamson, R.T.; Martin, G.E. Carbon Multiplicity Editing in Long-Range Heteronuclear Correlation NMR Experiments: A Valuable Tool for the Structure Elucidation of Natural Products. *J. Nat. Prod.* **2015**, *78*, 2236–2241, doi:10.1021/acs.jnatprod.5b00447.
21. Sørensen, O.W.; Dønstrup, S.; Bildsøe, H.; Jakobsen, H.J. Suppression of J cross-talk in subspectral editing. The SEMUT GL pulse sequence. *J. Magn. Reson.* **1983**, *55*, 347–354, doi:10.1016/0022-2364(83)90248-2.
22. Elyashberg, M.; Argyropoulos, D. Computer Assisted Structure Elucidation (CASE): Current and future perspectives. *Magn. Reson. Chem.* **2020**, doi:10.1002/mrc.5115.
23. Elyashberg, M. Identification and structure elucidation by NMR spectroscopy. *TrAC Trends Anal. Chem.* **2015**, *69*, 88–97, doi:10.1016/j.trac.2015.02.014.
24. Buevich, A.V.; Elyashberg, M.E. Synergistic Combination of CASE Algorithms and DFT Chemical Shift Predictions: A Powerful Approach for Structure Elucidation, Verification, and Revision. *J. Nat. Prod.* **2016**, *79*, 3105–3116, doi:10.1021/acs.jnatprod.6b00799.
25. Pupier, M.; Nuzillard, J.-M.; Wist, J.; Schlörer, N.E.; Kuhn, S.; Erdelyi, M.; Steinbeck, C.; Williams, A.J.; Butts, C.; Claridge, T.D.; et al. NMReDATA, a standard to report the NMR assignment and parameters of organic compounds. *Magn. Reson. Chem.* **2018**, *56*, 703–715, doi:10.1002/mrc.4737.
26. Elyashberg, M.; Argyropoulos, D. NMR-based Computer-assisted Structure Elucidation (CASE) of Small Organic Molecules in Solution: Recent Advances. *Emagres* **2019**, *8*, 239–253, doi:10.1002/9780470034590.emrstm1618.
27. Buevich, A.V.; Elyashberg, M.E. Enhancing computer-assisted structure elucidation with DFT analysis of J-couplings. *Magn. Reson. Chem.* **2020**, *58*, 594–606, doi:10.1002/mrc.4996.
28. Mateescu, G.D.; Valeriu, A. *2D NMR Density Matrix and Product Operator Treatment*; Prentice Hall: Hoboken, NJ, USA, 1993.
29. Bendall, M.R.; Pegg, D.T. Complete accurate editing of decoupled 13C spectra using DEPT and a quaternary-only sequence. *J. Magn. Reson.* **1983**, *53*, 272–296, doi:10.1016/0022-2364(83)90032-x.
30. Kögler, H.; Sørensen, O.; Bodenhausen, G.; Ernst, R. Low-pass J filters. Suppression of neighbor peaks in heteronuclear relayed correlation spectra. *J. Magn. Reson.* **1983**, *55*, 157–163, doi:10.1016/0022-2364(83)90285-8.
31. Furrer, J.; Guerra, S.; Deschenaux, R. Accordion-optimized DEPT experiments. *Magn. Reson. Chem.* **2011**, *49*, 16–22, doi:10.1002/mrc.2701.
32. Holman, M.A.; Williamson, N.M.; Ward, A.D. Preparation and Cyclization of Some N-(2,2-Dimethylpropargyl) Homo- and Heteroaromatic Amines and the Synthesis of Some Pyrido[2 ,3-d]pyrimidines. *Aust. J. Chem.* **2005**, *58*, 368–374, doi:10.1071/ch04260.

33. Majumdar, K.C.; Ganai, S. An expedient approach to substituted triazolo[1,5-a][1,4]benzodiazepines via Cu-catalyzed tandem Ullmann C–N coupling/azide-alkyne cycloaddition. *Tetrahedron Lett.* **2013**, *54*, 6192–6195, doi:10.1016/j.tetlet.2013.08.125.